418. Research of dynamics of the centrifugal ring coupling with the additional masses

B. Spruogis, V. Turla and E. Jurkonis
Vilnius Gediminas Technical University
Basanaviciaus 28, LT-03224, Vilnius, Lithuania
e-mail: *bs@ti.vgtu.lt   Vytautas.Turla@me.vgtu.lt   eugjurk@yahoo.com*

Abstract. Continuous increase of the rotational speed of the rotating machinery results in the inevitable growth of the dynamic loads and vibration. One of the most efficient way of absorbing vibration in the rotary systems is the application of the resilient couplings. The current paper is concerned with the dynamics of the pendulum-type centrifugal ring elastic coupling. The torque and stiffness characteristics as well as the stability areas of the coupling's operation are investigated. The compensational properties and effect of the vibration absorption of the coupling are analyzed.

1. Introduction

The structural scheme of the ring–form centrifugal coupling with the additional masses is shown in Fig. 1. The driving half–coupling is manufactured in the form of a hub 1 with two diametrically opposite stems 2 which have cylindrical holes oriented parallel with the axis of the shafts. Stems contain pins 3 on which centrifugal pendulums 4 are hinged. Two concentric centrifugal spiral springs 5 are attached rigidly to the pendulums with the help of the bolts 7 and gaskets 8. These springs possess different coils of relatively large diameter. Bolts 7 and gaskets 8 play the role of the centrifugal masses.

Driven half–coupling consists of the hub 9 with two diametrically opposite stems 10. Stems 10 are also connected with the centrifugal spiral springs 5 and 6 with the help of the gaskets 11 and bolts 12. Thus, the sections of the cylindrical spiral springs 5 and 6 are the connecting links between the half–couplings [1, 2, 4, 7].

The coupling operates in the following way. In static condition and rotation without load the stems 2 of the driving half–coupling and the stems 10 of the driven half–coupling are perpendicular to each other ($\alpha = 90^0$) and the axes of the coils of spiral springs (face projection) are almost ideal circles. While the driving coupling rotates with slow speed under the torsion load angle α increases due to the deflection of the centrifugal pendulums from the

radial position and deformation (complex bending) of the spring rings 5 and 6. At the higher speed centrifugal forces of the rotating masses grow up and centrifugal pendulums tend to return to the initial radial position. The return to the primary position of the whole system is also facilitated by the restoring elastic forces of the spring rings. The shift of the centrifugal masses (pendulums) from the rotation axis results in the rectification of the coils of the springs and the corresponding decrease of angle α. At the certain value of the torsion load and rotational speed we have the dynamic equilibrium of the system which is characterized by the deflection angle α and corresponding deformations of the spring rings.

2. Stationary operation of coupling

The present analysis starts with the determination of the main relationships. For this purpose potential and kinetic energy of the system is derived.

The dynamic model is presented in Fig. 2. We introduce three generalized coordinates: turn angle of the driven part of the coupling φ_1, turn angle of the driven part ing the coupling φ_2 and angle α_x defining the position of the radius–vector of the reduced mass m. R designates the radius of the initial elastic ring.

The third (additional) degree of freedom appears because of the ability of the system to deform, therefore

the coupling is able to twist without the change of the distance of mass m from rotation axis.
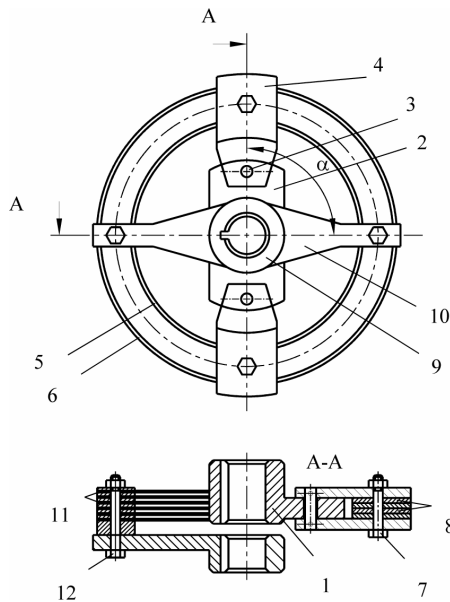

Fig. 1. Structural scheme of coupling: 1 – hub of the driving half-coupling; 2, 10 – stems of the corresponding half–couplings; 3 – pins; 4 – centrifugal pendulums; 5, 6 – spring rings; 7, 12 – connecting bolts; 8, 11 – gaskets, 9 – hub of the driven half–coupling.
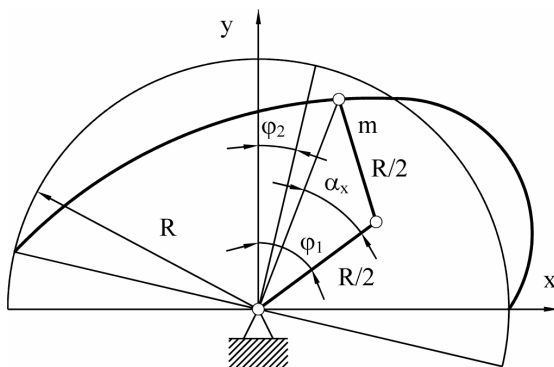

Fig. 2. Model of the coupling

Taking into account the symmetricity of the coupling the kinetic energy of the entire isolated two–mass system with the coupling according to [2] can be written as follows:

$$T = \frac{1}{2}I_1\dot{\varphi}_1^2 + \frac{1}{2}I_2\dot{\varphi}_2^2 + m\left[\begin{array}{c} R^2\dot{\alpha}_x^2 + (R\cos\alpha_x)^2\dot{\varphi}_1^2 - \\ -2(R\cos\alpha_x)^2\dot{\varphi}_1\dot{\alpha}_x \end{array}\right], \quad (1)$$

where I_1 and I_2 – constant moments of inertia of the driving and driven parts, respectively. The dot denotes the differentiation via time.

The model for the calculation of the potential energy of the half–ring is shown in Fig. 3, where δ_1 and δ_2

designate the displacement components of the fixed point A of the ring in the two perpendicular directions.

Using the technique given in [2] the potential energy of the whole ring is governed by the equation

$$\Pi = \frac{EI}{R^3} \cdot \frac{8(\pi^2 - 8)}{\pi^3 - 20\pi + 32}(\delta_1^2 + \delta_2^2) = $$
$$= 87(\delta_1^2 + \delta_2^2)\frac{EI}{R^3}, \quad (2)$$

where EI – bending stiffness of the ring.

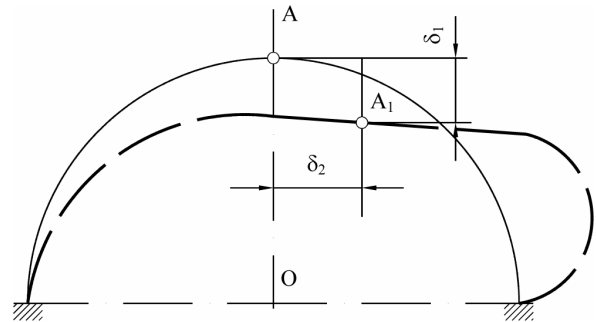**Fig. 3.** Model for the determination of the potential energy of the half–ring

For small displacements δ_1 and δ_2 can be expressed through generalized coordinates; potential energy of the system is a function of the generalized coordinates:

$$\Pi = 87\frac{EI}{R^3}\left[(\varphi_1 - \varphi_2 - \alpha_x)^2 + (1 - \cos\alpha_x)^2\right]. \quad (3)$$

The most convenient way to investigate the stationary rotation of the system is to use the averaged value of the varying part of the kinetic potential of the system [3] which has the form (the hyphen from above designates average value for one turn):

$$\bar{T} - \bar{\Pi} = m(R\cos\bar{\alpha}_x)^2\omega^2 - 87\frac{EI}{R^3}\left[\begin{array}{c}(\bar{\psi} - \bar{\alpha}_x)^2 + \\ + (1 - \cos\bar{\alpha}_x)^2\end{array}\right]. \quad (4)$$

As seen the averaged value of the kinetic potential of the system is the function of two averaged deflections: the full averaged deflection of the coupling $\bar{\psi}$ and additional deflection of the coupling $\bar{\alpha}_x$.

In this case the characteristic of the coupling is determined by the system of the two equations [4]:

$$-\frac{\partial(\bar{T} - \bar{\Pi})}{\partial\bar{\psi}} = \bar{M},$$
$$-\frac{\partial(\bar{T} - \bar{\Pi})}{\partial\bar{\alpha}_x} = 0. \quad (5)$$

566

Specifically for this coupling (N is number of coils)

$$\bar{M} = 174N \frac{EI}{R} \left(\bar{\psi} - \bar{\alpha}_x \right),$$

$$\bar{M} = mR^2 \omega^2 \sin 2\bar{\alpha}_x + 174N \frac{EI}{R} \left(\sin \bar{\alpha}_x - \frac{1}{2} \sin 2\bar{\alpha}_x \right). \quad (6)$$

Graphical interpretation of the characteristic of the coupling in the common sense (the dependence of the torque on the total deformation) is shown in Fig. 4. It was obtained using equation (6).

It's obvious that the physical model of the coupling can be represented by the two sequentially connected springs – linear spring

$$C_1 = 174N \frac{EI}{R} \quad (7)$$

and nonlinear spring

$$C_2 = 2mR^2 \omega^2 \cos 2\alpha_x + 174 \frac{EI}{R} \left(\cos \bar{\alpha}_x - \cos 2\bar{\alpha}_x \right). \quad (8)$$

Hence the reduced total stiffness is:

$$C_n = \frac{2mR^2 \omega^2 \cos 2\alpha_x + 174 \frac{EI}{R} \left(\cos \bar{\alpha}_x - \cos 2\bar{\alpha}_x \right)}{\frac{mR^3 \omega^2}{87NEI} \cos 2\bar{\alpha}_x + \cos \bar{\alpha}_x - \cos 2\bar{\alpha}_x + 1}. \quad (9)$$

Naturally, in the area of small deformations the characteristic of the coupling can be well approximated by the linear function of the summed deformation, that is:

$$\bar{M} = C_n \left(\varphi_1 - \varphi_2 \right). \quad (10)$$

Let's verify the stability of the deformed system. This requires to find the maximum of the averaged kinetic potential of the system [5] as a function of the two variables ($\bar{\psi}$ and $\bar{\alpha}_x$).

Obviously in this particular case the existence of maximum leads to the unique condition [6]:

$$\begin{vmatrix} \dfrac{\partial^2 \left(\bar{T} - \bar{\Pi} \right)}{\partial \bar{\psi}^2} & \dfrac{\partial^2 \left(\bar{T} - \bar{\Pi} \right)}{\partial \bar{\psi} \cdot \partial \bar{\alpha}_x} \\[4mm] \dfrac{\partial^2 \left(\bar{T} - \bar{\Pi} \right)}{\partial \bar{\psi} \cdot \partial \bar{\alpha}_x} & \dfrac{\partial^2 \left(\bar{T} - \bar{\Pi} \right)}{\partial \bar{\alpha}_x^2} \end{vmatrix} \rangle \ 0 \quad (11)$$

or specifically for this coupling

$$umR^2\omega^2 \cos 2\bar{\alpha}_x + 87NEI \left(\cos \bar{\alpha}_x - \cos 2\bar{\alpha}_x \right) \rangle \ 0, \quad (12)$$

where $u = R - OA_1$ (Fig. 2 and 3).

Inequality (12) is simultaneously the condition of the positive value of the stiffness C_2, and of the positive value of the total stiffness of the coupling C_M as well. The boundaries of the stable deformation area of the coupling mainly depend on the ration between the rotational speed and the parameters of the coupling and are determined from the inequality:

$$\left(\cos \bar{\alpha}_x + \frac{1}{S} \sqrt{\frac{1}{S^2} + \frac{1}{2}} \right)\left(\cos \bar{\alpha}_x + \frac{1}{S} - \sqrt{\frac{1}{S^2} + \frac{1}{2}} \right) \rangle \ 0, \quad (13)$$

where $S = 4\left(\dfrac{R}{87EI} m\omega^2 - 1 \right)$.

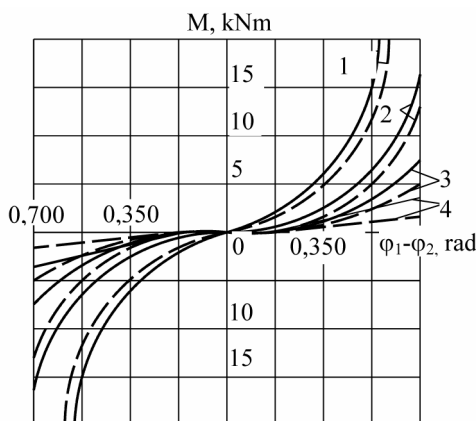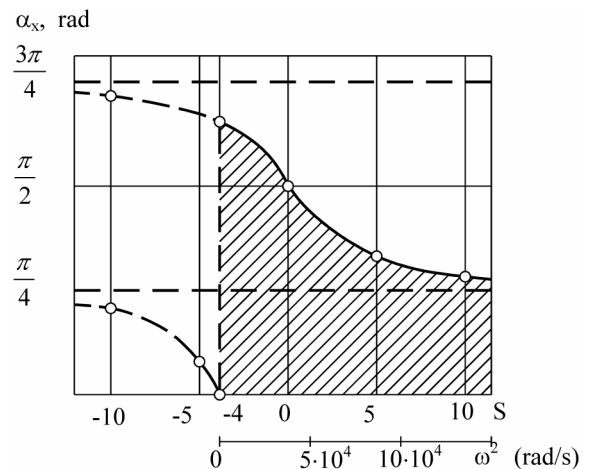Graphical interpretation of the stable area of the deformation of the coupling is given in Fig. 5.

Fig. 4. Characteristic of the coupling at R=125 mm, N=20 (coils), m=2 kg; continuous and dashed curves correspond to n=2200 rpm and n=500 rpm, respectively; 1 – d=5 mm; 2 – d=4 mm; 3 – d=3 mm; 4 – d=2 mm, where d is the wire diameter

Fig. 5. Area of the stable deformation of coupling at m=1 kg, R=125 mm and d=3 mm

567

3. Compensating properties of coupling

Angular and axial stiffness is determined according to [7].

In the analysis of the radial stiffness two limit cases must be encountered. In the first case the force acting on the coupling in the radial direction coincides with the radial axis (Fig. 1) passing through the fixing center of the elastic ring, bolt 7, pins 3 of the pendulums 4 and the center of the coupling. In this case the radial component of the coupling stiffness is expressed by the following formula [5]:

$$C_r = 174 \frac{EI}{R^3} - 2m\omega^2 A^2 \sin^2\left(\gamma_0 + \delta_0\right), \qquad (14)$$

where γ_0 – angle characterizing the location of the plain of the shift of the connected axes with respect to the links of PRCC; in this particular case $\delta_0 = -0,12\pi$, $A = 1,2233$.

In the second case the radial force is perpendicular to the axis passing through the bolts 7, pins 3 of the pendulums 4 and the center of the coupling.

In this case the stiffness of the coupling depends on the displacement value (misalignment of the shafts e). Its elastic component is approximately expressed by:

$$C_{min} \cong C_{max} \frac{e}{R}. \qquad (15)$$

For the estimation of the total radial stiffness of the coupling without the twist of an arbitrary angle we use the following expressions:

$$C'_{max} = C_{max} - 2m\omega^2 ,$$
$$C'_{min} = C_{min} + 4m\omega^2 . \qquad (16)$$

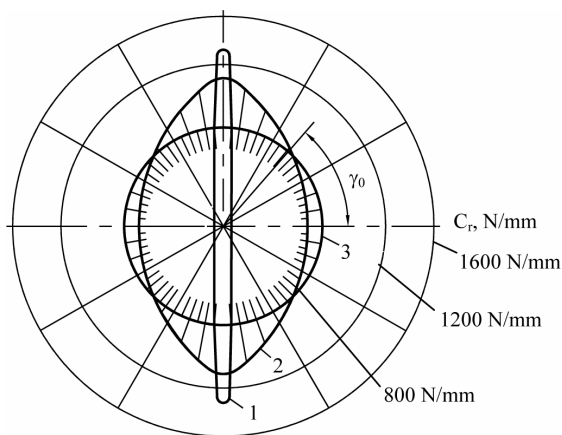The cyclogram of the radial stiffness is shown in Fig. 6.

Fig. 6. Radial stiffness of coupling at R=125 mm, d=3 mm, N=24, m=2 kg and prescribed misalignment e=2,5 mm as a function of the angular direction: curves 1, 2 and 3 correspond to ω=0, ω=300 rad/s and ω=342 rad/s, respectively

The spectral densities of the oscillations of the motor crankshaft and intermediate shaft are presented in Fig. 8.

It can be seen from the above curves that the intermediate shaft beyond coupling vibrates with the smaller amplitude. The variance of the oscillations of the intermediate shaft is two times smaller than the variance of the crankshaft vibration.

The evaluation of the compensating properties of the coupling in dynamics is illustrated in Fig. 7.

Vibration oscillograms were processed on the computer [8, 9, 10].

4. Torsion vibration of the system with coupling

For the derivation of the equations governing the small oscillations we use the expressions (1) and (2). If the isolated system is considered [6] nonlinear equations of motion are:

$$\ddot{\varphi}_1\left(I_1 + 2mR^2\cos^2\alpha_x\right) - \ddot{\alpha}_x mR^2\cos^2\alpha_x -$$
$$-\dot{\varphi}_1 4mR^2\cos\alpha_x\sin\alpha_x + \dot{\alpha}_x^2 4mR^2\cos\alpha_x\sin\alpha_x +$$
$$+4HR^2\left(\varphi_1 - \varphi_2 - \alpha_x\right) = M_1 ,$$
$$\ddot{\varphi}_2 I_2 - 4HR^2\left(\varphi_1 - \varphi_2 - \alpha_x\right) = -M_2 , \qquad (17)$$
$$\ddot{\alpha}_x 2mR^2 - \ddot{\varphi}_1 2mR^2\cos^2\alpha_x + \dot{\varphi}_2 2mR^2\cos\alpha_x\sin\alpha_x -$$
$$-4HR^2\left(I_1 - \varphi_2 + 2\alpha_x - \cos\alpha_x - \cos\alpha_x\sin\alpha_x\right) = 0 .$$

Using the expressions

$$\varphi_1 = \alpha_1 + \omega t + \beta_1 ,$$
$$\varphi_2 = \alpha_2 + \omega t + \beta_2 , \qquad (18)$$

and taking into account that $\alpha_x = \alpha_0 + x$ (x – deviation) and expanding the coefficients of equation (17) into the power series we come to the system of the three nonlinear differential equations governing the small oscillations of the driving and driven parts in the vicinity of the stationary motion:

$$\left(I_1 + 2mR^2\cos^2\alpha_x\right)\ddot{\beta}_1 - 2mR^2\cos^2\alpha_x \cdot \ddot{x} -$$
$$-2mR^2\omega\sin 2\alpha_x \cdot \dot{x} + 4HR^2\beta_1 - 4HR^2\beta_2 +$$
$$+4HR^2 x = m_1\left(t\right) ,$$
$$I_2\ddot{\beta}_2 - 4HR^2\beta_1 + 4HR^2\beta_2 + 4HR^2 x = m_2\left(t\right) , \qquad (19)$$
$$2mR^2\ddot{x} - 2mR^2\cos^2\alpha_x \cdot \ddot{\beta}_1 + 2mR^2\omega\sin 2\alpha_x \cdot \dot{\beta}_1 +$$
$$+\left(4HR^2 + 2HR^2\cos\alpha_x - 4HR^2\sin\alpha_x\right)x -$$
$$-4HR^2\beta_1 + 4HR^2\beta_2 = 0 ,$$
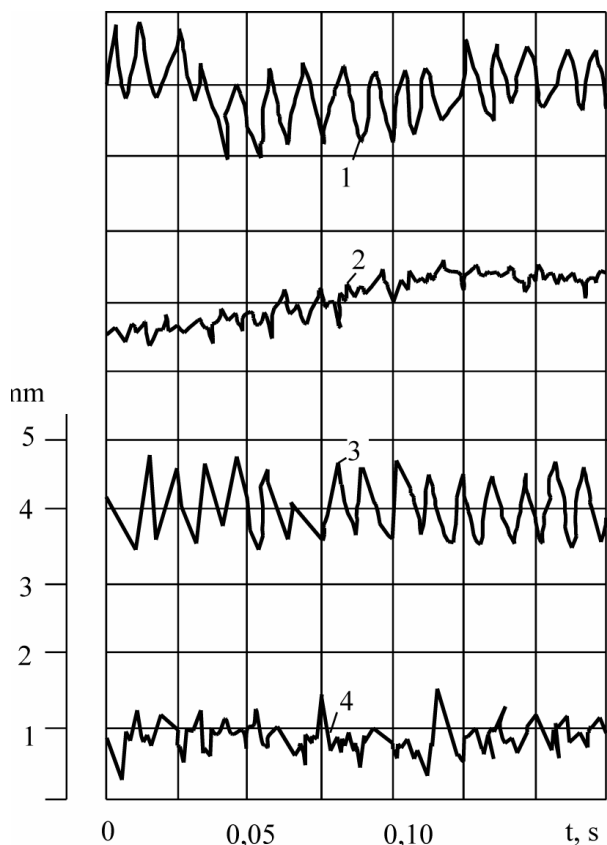
where $H = 43,5\dfrac{EI}{R^3}$.

568

Fig. 7. Values of the radial vibrational displacements and the beating of the shaft in experimental test of coupling on the stand with motor (load 500 Nm, speed 1200 rpm): 1 – vibration of the motor casing, 2 – vibration of the casing of the intermediate support, 3 – beating of the crankshaft, 4 – beating of the intermediate shaft

Fig. 8. Spectral density of vibration: a – of the crankshaft ($D=0.21779$ mm^2), b – of intermediate shaft ($D=0.07256$ mm^2); here D – variance, S_1 – spectral density, f – oscillation frequency

Theoretical and experimental analysis shows that the coupling is vibration–resistant, especially in case of torsion oscillations. This is shown in Fig. 9.

Below we resume the investigation of the antivibrational properties of the coupling based on the analysis of the system of three equations (19) and experimental data.

The additional degree of freedom positively influences the compensation of the starting and torsion dynamic loads. Considering this criterion the optimal choice of the parameters of the coupling is a separate task.

Incorporation of the coupling into any rotating system gives the effect of the tracking tuning: all curves of the natural frequencies in the function of the angular speed have the tendency to increase. This allows to expel the resonance frequencies out of the operating range of the system.

Considering the isolation of torsion vibration it should be noted that the additional degree of freedom makes the coupling a reliable vibration-isolating device in the wide range of excitation frequencies. The area of the excitation frequencies lying beyond the highest natural frequency of the system is considered here. This is expressed by:
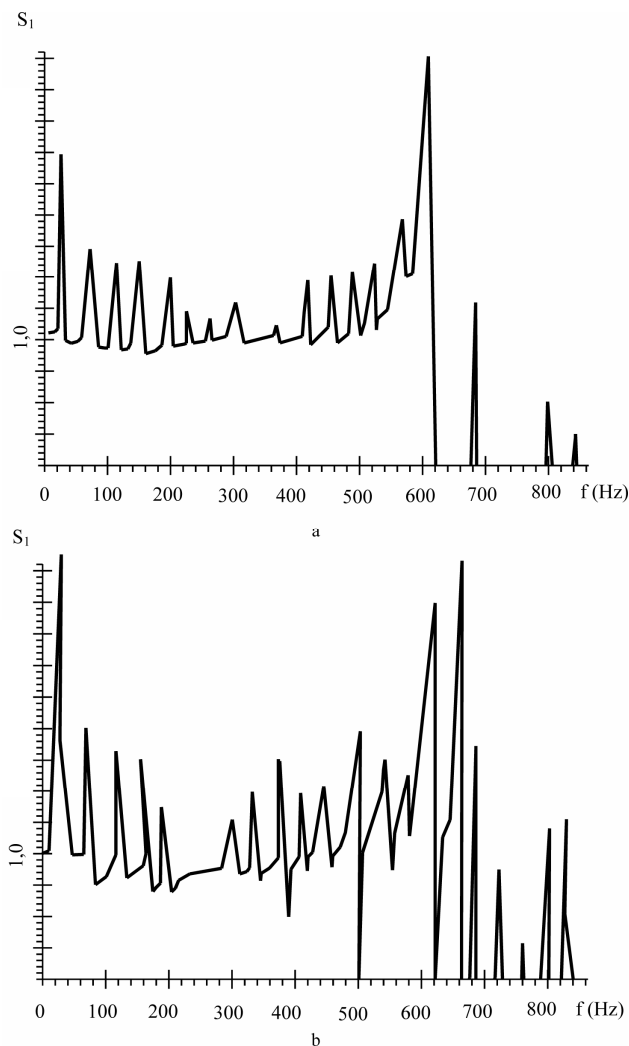
$$\lim_{p_b \to \infty} \zeta = 0, \tag{20}$$

where ζ – coefficient of the transformation of the harmonic force, and p_b – frequency of the external excitation.

Practically it's possible to achieve that all real frequencies in the stationary rotation become close to "infinitely large" and are filtered almost ideally.

The effect of the vibration absorption obtained according to the feedback principle is almost independent of the additional degree of freedom. It's known that each half–coupling acts on the other one as a vibration absorber and this can be very effective at resonance tuning. As the resonance tuning due to the locality of the effect practically can't play the substantial role, we estimate the effect of the vibration absorption in the areas lying "slightly below" and "slightly above" the resonance frequencies. Note that in

569

these areas the efficiency of the standard couplings is practically equal to zero. In our case the effect of the driven part on the driving one is determined from the following expressions:

$$\lim_{p_b \to 0} I_e = I_f + \frac{1}{\omega^2} \frac{4\left(\partial T / \partial \bar{\alpha}_x\right)^2}{\partial^2 \left(\bar{T} - \bar{\Pi}\right) / \partial \bar{\alpha}_x^2} = I_f + \frac{4M_T^2}{C_M \omega^2}, \quad (21)$$

$$\lim_{p_b \to \infty} I_e = \frac{1}{2} mR^2 \sin^2 2\alpha_x, \quad (22)$$

where M_T – torque component caused by the centrifugal forces, C_M – total stiffness of the coupling, I_e – equivalent moment of inertia of the driven part of the coupling and I_f – physical moment of inertia.
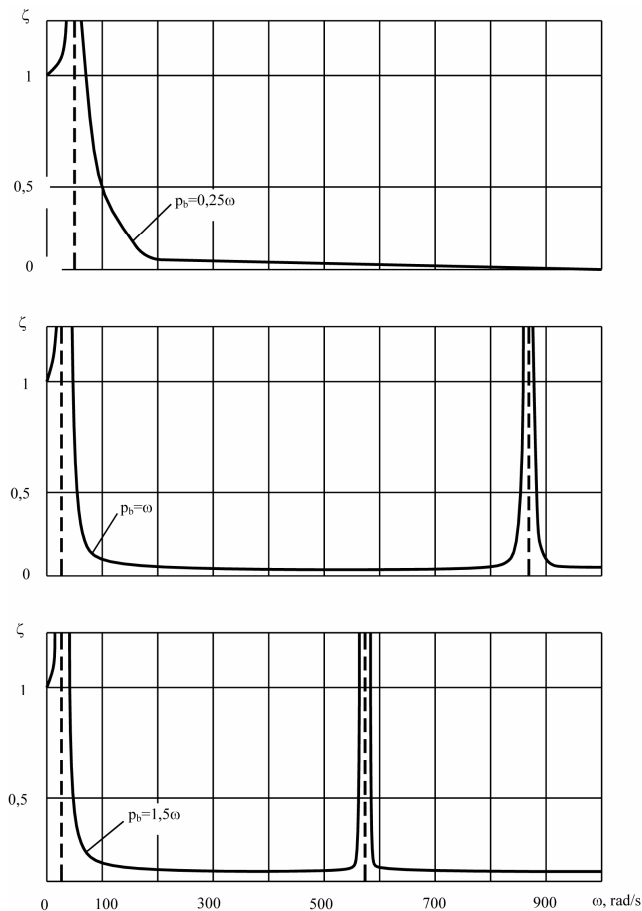

Fig. 9. Coefficient of the transformation of the harmonic force of coupling in case of mass excitation: R=125 mm, m=1 kg, N=20 (coils), d=3 mm and $J_l/N = 4{,}5 \cdot 10^{-4}$ s^2.

5. Conclusion

Adding an additional degree of freedom into the coupling considerably increases its vibration–isolating and compensating properties. The other characteristics of the coupling doesn't change or vary very little. Of course, the additional degree of freedom is only a resonance, but practically in the well designed structure all resonances can be moved out of the operating area.

References

1. **Kavolėlis A.–P., Jurevič J. and Spruogis B.** Operation Analysis of the Special Coupling with the "Additional" Degree of Freedom. *Transactions of the Higher Schools, Mashinostroenie.* Vol.10. 1976. P.25–28.
2. **Kavolėlis A.–P. and Ragulskis K.** Rotating System with the Dynamic Link of the Centrifugal–Inertia Type.–In: Self–Synchronization of Mechanical Systems (Part 2. Self–synchronization, Modelling). Vilnius: Mintis, 1967.
3. **Kavolėlis A.–P. and Spruogis B.** Unique Dynamic Devices for Rotary Motion Transmission by Spring Rings. *Synopsis Fourth World Congress on the Theory of Machines and Mechanisms,* Newcastle upon Tyne. England, 1975.
4. **Spruogis B.** The devices of transmission and stabilization of rotary motion. V.: Technika, 1997. 476 p. (in Russian).
5. **Bogdevičius M., Spruogis B.** Theoretical investigations into rotary systems with elastic link caused by the deflection of the shafts // *Transportas (Transport Engineering).* V.: Technika, 1996. No2(13). p. 70–81 (in Russian).
6. **Bogdevičius M., Spruogis B.** Dynamic and mathematical models of rotor system with elastic link in the presence of shafts misalignment // *2nd International Conference of Mechanical Engineering "Mechanics'97".* Proceedings. Part 1. Vilnius: Technika, 1997. p. 78–84.
7. **Ragulskis K., Spruogis B., Ragulskis M.** Transformation of rotational motion by inertia couplings. Vilnius: Technika, 1999. 236 p.
8. **Bogdevičius M.** Simulation of Dynamic Processes in Hydraulic, Pneumatic and Mechanical Drivers and their Elements. Vilnius: Technika, 2000. 96 p.
9. **Aladjev V., Bogdevičius M.** Maple 6: Solution of the Mathematical, Statistical and Engineering – Physical Problems. Moscow: *Laboratory of Basic Knowledges*, 2001. 824 p. (in Russian).
10. **Bogdevičius M.** Simulation of dynamic processes in mechanical drive with coupling gas // *Proceedings of the Six International Conference on Motion and Vibration Control*, August 19–23, 2002, Saitama, Japan, p.543–546.